Protein Dielectrophoresis in Solution

Journal:	*The Journal of Physical Chemistry*
Manuscript ID	jp-2018-06864g.R1
Manuscript Type:	Article
Date Submitted by the Author:	n/a
Complete List of Authors:	Seyedi, Salman; Arizona State University, Physics Matyushov, Dmitry; Arizona State University, School of Molecular Sciences

Protein Dielectrophoresis in Solution

Salman S. Seyedi† and Dmitry V. Matyushov *,‡

†*Department of Physics, PO Box 871504, Tempe, AZ 85287-1504*
‡*Department of Physics and School of Molecular Sciences, Arizona State University, PO Box 871504, Tempe, AZ 85287-1504*

E-mail: dmitrym@asu.edu, Tel:(480)965-0057

Abstract

Proteins experience either pulling or repelling force from the gradient of an external electric field due to the effect known as dielectrophoresis (DEP). The susceptibility to the field gradient is traditionally calculated from the solution of the electrostatic boundary-value problem, which requires assigning a dielectric constant to the protein. This assignment is essential since the DEP susceptibility is proportional, in dielectric theories, to the Clausius-Mossotti factor, the sign of which is controlled by whether the protein dielectric constant is below (repelling) or above (pulling) the dielectric constant of water. Dielectric constant is not uniquely or even well defined for a particle of molecular size and the Clausius-Mossotti factor is shown here to be inadequate for describing the dipolar response of the protein and hydration water. An alternative theory is developed from the standpoint of molecular properties of the protein solute and water solvent. The effective polarity of the protein molecule enters the theory in terms of the variance of its molecular dipole moment and its refractive index. Molecular dynamics (MD) simulations of the protein cytochrome *c* in solution are performed to calculate the dipolar susceptibilities entering the theory. We find that tumbling of the protein on the nanosecond time-scale results in a positive DEP (pulling). The DEP susceptibility for cytochrome *c* acquired from MD simulations is $10^3 - 10^4$ times higher than predicted by the Clausius-Mossotti factor. Nevertheless, this high DEP susceptibility is fully consistent with empirically confirmed Oncley's equation connecting the protein dipole to dielectric increments of protein solutions. For cytochrome *c*, high DEP susceptibilities calculated from MD are consistent with experimental dielectric data. We provide a general relation connecting the DEP susceptibility to the dielectric increment of solution.

Introduction

Dielectrophoresis (DEP) is the phenomenon responsible for a force acting on a particle, often in solution, from a nonuniform electric field. The DEP force is a consequence of the dependence of the free energy of a particle on its position in a nonuniform external field. If $\langle \mathbf{M} \rangle_E$ is the combined average dipole moment induced in the solute and in the solute-solvent interface by the (vacuum) field of external charges $\mathbf{E}_0$ (Figure 1), the free energy of polarizing the solute becomes[1,2]

$$\mathcal{F}_{\mathrm{DEP}} = -\tfrac{1}{2}\langle \mathbf{M} \rangle_E \cdot \mathbf{E}_0 \qquad (1)$$

Here, $\langle \dots \rangle_E$ refers to an ensemble average calculated in the presence of the external field.

Since weak fields are employed in experiments, linear response holds and $\langle \mathbf{M} \rangle_E$ is proportional to $\mathbf{E}_0$. The proportionality coefficient can be identified with the combined dipolar susceptibility of the solute and its interface with the liquid. One then proceeds to define the DEP force as the negative gradient of the free energy, with the result

$$\mathbf{F}_{\mathrm{DEP}} = \frac{3\Omega_0}{8\pi\epsilon_s} K \nabla E_0^2 \qquad (2)$$

Here, we have used the notations usually adopted in the literature,[3–5] with Ω_0 standing for the volume of the solute and ϵ_s for the dielectric constant (relative permittivity) of the solvent. Note that if the field is induced in a plane capacitor with applied voltage V, it defines the Maxwell field $E = V/d$ (d is the distance between the plates), with a simple connection $E = E_0/\epsilon_s$. Establishing the connection between $\mathbf{E}$ and $\mathbf{E}_0$ requires solving the dielectric boundary-value problem for more complex geometries. Finally, K in eq 2 is the DEP susceptibility. The parameters in eq 2 are chosen in a such a way that K produces the Clausius-Mossotti factor when continuum electrostatics is used to calculate the induced dipole moment

$$K = \frac{\epsilon_0 - \epsilon_s}{\epsilon_0 + 2\epsilon_s} \qquad (3)$$

Here, ϵ_0 is the dielectric constant assigned to the solute.

The basic prediction of eq 3 is the distinction between particles more or less polarizable than the surrounding solvent. If the particle is less polarizable, $\epsilon_0 < \epsilon_s$, the DEP is negative and the solute is repelled from the field gradient. In the opposite limit of the solute more polarizable than the solvent, $\epsilon_0 > \epsilon_s$, it is attracted to the field gra-

dient. While this picture is likely to be correct for sufficiently large solutes, the dielectric constant ϵ_0 can be reliably defined for macroscopic materials only. Even for solutes of the mesoscopic size (from tens of nm to μm), the surface polarization does not necessarily follow the standard assumptions of the theory of dielectrics. In addition to the surface ionic conductivity and polarization, a common complication,[3,6] the surface polarization caused by the solvent dipoles does not necessarily follow the standard boundary-value problem for two macroscopic dielectrics in contact.[7] How the surface polarization is modified compared to the standard predictions for the protein-water interface and what are the observable consequences of such changes are still mostly open questions.

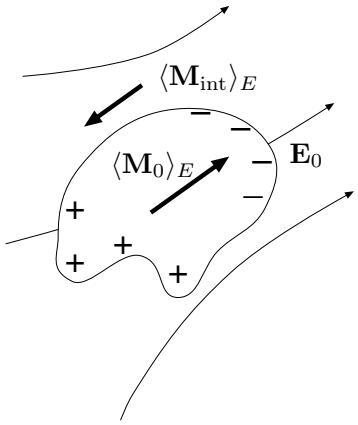

Figure 1: Schematic representation of the solute in the inhomogeneous external field $\mathbf{E}_0$. The overall dipole induced by the field $\langle \mathbf{M} \rangle_E$ is a sum of the solute dipole $\langle \mathbf{M}_0 \rangle_E$ and the interface dipole $\langle \mathbf{M}_{\rm int} \rangle_E$: $\langle \mathbf{M} \rangle_E = \langle \mathbf{M}_0 \rangle_E + \langle \mathbf{M}_{\rm int} \rangle_E$ The pluses and minuses at the dividing solute-solvent surface indicate the surface charge density[1] produced by a discontinuity in a polarized dielectric, which are responsible for $\langle \mathbf{M}{\rm int} \rangle_E$.

For objects of molecular size, ϵ_0 is not well defined from the theoretical standpoint[8,9] and in most cases cannot be measured experimentally.[10] There is a clear need for a theory based on molecular properties of the solute. Developing such a theory for proteins in solution is the goal of this study. Most importantly, we show that eq 3 does not describe the DEP of proteins. Even for positive DEP, the highest value of K, achieved at $\epsilon_0 \to \infty$, is $K = 1$. In contrast, our present simulations confirm an early result[11] that K far exceeds this number, reaching $K \simeq 10^4$ in simulations of proteins in water in the absence of electrolyte. Proteins in aqueous solutions should thus show a much greater DEP than predicted by eq 3 solely on the ground of dielectric theories.

The possibility of measuring DEP for molecular objects of the size of a soluble protein has been demonstrated in recent years by a number of studies[12–14] (see refs 15–17 for recent reviews). However, the magnitude of the DEP susceptibility for proteins has not been measured. Stronger DEP effect then predicted by eqs 2 and 3 was observed in ref 12, but the origin of this enhancement has remained unknown. Even the sign of the DEP effect for proteins has not been clearly established: both negative[13] and positive[18] signs of DEP susceptibilities have been reported. Here we address these issues to clarify the value of the DEP effect that should be expected for proteins in aqueous solutions.

Proteins typically possess a relatively large density of surface charge[19] required for their solubility. The negative and positive charges mostly compensate each other[20] to produce a typically negative overall charge of the protein at physiological conditions (cytochrome *c* studied here is, however, positively charged). The non-spherical shape of the molecule and incomplete compensation between the charges result in an overall large dipole moment of the protein of several hundreds of debye units when calculated relative to its center of mass.[20–26] For instance, the dipole moment of cytochrome *c* considered here is in the range $M_0 \simeq 250 - 400$ D depending on protein's net charge.[27] Fluctuations of orientations of this large dipole moment are related to protein's tumbling occurring on the typical time-scale of $\sim 10-20$ ns.[28] Since these times are much shorter than the observation times of the DEP, these librations of a relatively large molecular dipole moment lead to a large effective polarity of the protein molecule.

The polarity of a polar material is gauged in theories of dielectrics by the dipolar parameter[29,30] $y = (4\pi/9)\beta m^2 \rho$, where m is the molecular dipole, ρ is the number density of the dipoles, and $\beta = (k_{\rm B}T)^{-1}$ is the inverse temperature. For a single

protein molecule this parameter becomes[31]

$$y_0 = \frac{4\pi}{9}\beta\Omega_0^{-1}\langle(\delta\mathbf{M}_0)^2\rangle \quad (4)$$

where the deviation of the protein dipole moment from its average (usually zero) value, $\delta\mathbf{M}_0 = \mathbf{M}_0 - \langle\mathbf{M}_0\rangle$, is taken to determine the variance. If this parameter is considered as a gauge of polarity, a typical globular protein has $y_0 \simeq 10-60$, significantly exceeding $y \simeq 6$ for bulk water. Based on these estimates, suggesting that a typical protein should be more polarizable than surrounding water, one would expect a positive DEP for proteins in solutions, in agreement with more detailed calculations presented below. Low dielectric constants typically reported for protein powders might be misleading for the DEP calculations since proteins do not fully develop their surface ionization configurations at those conditions[9,32] and, potentially more importantly, tumbling of the protein dipole is suppressed in the powder samples.[33]

The outline of the paper is as follows. We first start with a general theory of molecular DEP, followed by the results of molecular dynamics (MD) simulations and by discussion of the results. We then connect the DEP experiment to dielectric spectroscopy of the protein solutions. More specifically we show that the DEP susceptibility $K(\omega)$, measured at the frequency ω, is related to the dielectric increment of the solution over bulk solvent by a simple equation

$$K(\omega) = \frac{\Delta\epsilon(\omega)}{\eta_0}\,\frac{2\epsilon_s(\omega)^2+1}{9\epsilon_s(\omega)} \quad (5)$$

Here, η_0 is the volume fraction of protein molecules in solution and $\Delta\epsilon(\omega)$ is the increment of the frequency-dependent dielectric function of solution over that of the solvent, $\epsilon_s(\omega)$. The DEP susceptibility and the dielectric function refer to the same frequency ω of the applied field of external charges $E_0(\omega)$. The ratio $\Delta\epsilon(\omega)/(3\eta_0)$ thus establishes the linear slope of the dielectric increment with the volume fraction of the solutes.[5,34]

Equation 5 is very significant from the practical standpoint as the potential source of calibration of DEP susceptibilities. It provides an independent access to the DEP susceptibility of proteins from dielectric spectroscopy of solutions. A significant practical appeal of this connection is that dielectric measurements give an integrated account of both the dipolar and electrolyte components of the response (at sufficiently high frequencies), which is currently challenging to calculate from numerical simulations[8] (see below).

General theory

We first consider a general particle of arbitrary shape and volume Ω_0 dissolved in a polar liquid with the dielectric constant ϵ_s (Figure 1). This particle is placed in a spatially nonuniform electric field $\mathbf{E}_0(\mathbf{r})$ created by external charges. The field changes on the length-scale significantly exceeding the size of the molecule and can be considered as locally constant. We therefore drop the spatial dependence and put $\mathbf{E}_0(\mathbf{r}) = \mathbf{E}_0$. The external field aligns the dipole moment of the solute, thus creating an average dipole moment along the field

$$\langle\mathbf{M}_0\rangle_E = \chi_0\Omega_0\mathbf{E}_0 \quad (6)$$

where χ_0 is the dipolar susceptibility of the solute.

The polarization of the solute dipole is not the only effect of the external electric field. Since the solute-solvent interface does not coincide with the equipotential surface of the external field, an inhomogeneous polarization of the interface is induced by the field in addition to aligning the solute dipole. The origin of this polarization is easiest to understand in the case of zero solute dipole, i.e., for a void in a polar liquid. In the case of the void, the surface charges in the polarized dielectric next to the dividing surface lead to an effective dipole moment of the interface opposite in the direction to the external electric field. This is illustrated in Figure 2.

The electrostatic field of external charges is not sufficiently strong to permanently orient dipoles of the liquid. However, when molecular dipoles, in the course of thermal motion, cross the interfacial dividing (dielectric) surface, their dipole moments are more often oriented along the external field, which is the only field of charges present in the problem. This dynamic stationary condition is represented by an effective static surface charge with the negative an positive lobes (Figure 2). For a

spherical void, the solution of the standard dielectric boundary-value problem leads to the following interface dipole[1,2]

$$\mathbf{M}_{\text{int}} = -\frac{3\Omega_0}{2\epsilon_s + 1}\mathbf{P} \tag{7}$$

where $\mathbf{P}$ is the uniform polarization density induced in the bulk dielectric by the uniform external field.[1]

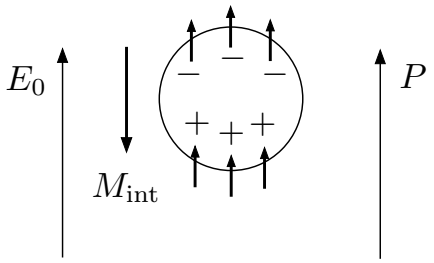

Figure 2: Schematic representation of the interfacial polarization of a void placed in the locally homogeneous external field $\mathbf{E}_0$. The arrows indicate dipoles of the solvent arriving in the interface with preferential orientation dictated by the external field. The interface dipole $\mathbf{M}_{\text{int}}$ is formed by the surface charge density representing the alignment of the interfacial dipoles.[1] The uniform polarization density of the dielectric induced by the external field is P.

The physical meaning of this result is straightforward, and it helps to understand possible pitfalls of extending this line of thought to more complex situations. The dipole moment $\mathbf{M}_{\text{int}}$ in eq 7 describes the reduction of the sample polarization by introducing voids into it. For an ideal solution of N_0 voids, polarization of the bulk liquid is reduced by the term $N_0\mathbf{M}_{\text{int}}$. The induction of the surface charge in the interface (Figure 2) is responsible for the difference between the electrostatic result in eq 7 and the naive assumption assigning the reduction of the dipole moment to the volume eliminated from the polarized dielectric $-N_0\Omega_0\mathbf{P}$. This naive approach, disregarding the non-additive surface polarization in the interface, leads to representing the absorption coefficient of a solution by a volume-weighted sum of component absorption coefficients.[35,36] This deficiency was corrected in refs 37 and 38.

When the dipole moment $\mathbf{M}_{\text{int}}$ is used in eq 1 along with the assumption that $\mathbf{P}$ is created by polarizing a dielectric slab in the plane capacitor, $\mathbf{P} = (\epsilon_s - 1)/(4\pi\epsilon_s)\mathbf{E}_0$, one arrives at eq 3 with $\epsilon_0 = 1$ corresponding to a non-polarizable void. This is the case of a negative DEP when the dipole moment induced in the interface is opposite to the external field and leads to the repulsion of the solute from the field gradient. A more general case of a void filled with the dielectric is obtained by noting that the dielectric boundary-value problem is sensitive only to the ratio of two dielectric constants at the interface ϵ_s/ϵ_0. Therefore, the void problem is equivalent to the case of an arbitrary dielectric constant assigned to the spherical solute when ϵ_s/ϵ_0 is used for the solvent. Equation 3 then follows from eq 7.

Before we proceed to a more general case of the solute carrying its dipole moment and then to a realistic hydrated protein, it is useful to point out potential pitfalls of the physical picture illustrated in Figure 2. The assignment of the interfacial surface charge to dipoles arriving to the interface with preferential orientations determined by the external field can be strongly modified by the interfacial structure of the solvent. For instance, adopting Figure 2, let's imagine that the orientation of the dipole pointing outward from the void is strongly disfavored by the structure of the interface, but dipoles pointing toward the void are favored instead. In such interfaces, the positive lobe of the surface will form, but the negative lobe will be strongly suppressed. The interface will then behave as a monopole and the solute can display mobility even in a uniform external field.[39] One also has to keep in mind that surface charges of the solute (ionized residues of the protein) will create their own orienting fields and thus impose orientational structure of the interfacial water. The surface charge density assigned to the dividing surface will then reflect the distribution of the solute charge close to the interface.

When the nonuniform distribution of the molecular charge of the solute is approximated by a point dipole moment, the total dipole moment induced by the external field becomes a sum of the solute's permanent dipole preferentially aligned along the field and the dipole of the polarized interface (Figure 1)

$$\langle\mathbf{M}\rangle_E = \langle\mathbf{M}_0\rangle_E + \langle\mathbf{M}_{\text{int}}\rangle_E \tag{8}$$

Here, in contrast to the case of a void, we have

added angular brackets to the interface dipole to stress that it is now determined by the combined effect of the external field and the field of the solute. Given that the latter fluctuates due to thermal motion, only the average value of the interface dipole is considered. Further, one can define the susceptibility of the interface in analogy with eq 6 as follows

$$\langle \mathbf{M}_{\text{int}} \rangle_E = \chi_{\text{int}} \Omega_0 \mathbf{E}_0 \tag{9}$$

The solute susceptibility χ_0 in eq 6 follows directly from the static limit of the linear response approximation[40] as

$$\chi_0 = \frac{\beta}{3\Omega_0} \langle \delta\mathbf{M}_0 \cdot \delta\mathbf{M} \rangle \tag{10}$$

Here, the angular brackets without the subscript denote an ensemble average in the absence of an external electric field. Further, in eq 10, $\mathbf{M} = \mathbf{M}_0 + \mathbf{M}_s$ is the instantaneous total dipole moment of the sample, including the dipole moment of the solute, $\mathbf{M}_0$, and the dipole moment of the solvent, $\mathbf{M}_s$.

The solute dipolar susceptibility χ_0 can be contrasted with the self susceptibility

$$\chi_{00} = \frac{\beta}{3\Omega_0} \langle (\delta\mathbf{M}_0)^2 \rangle \tag{11}$$

which does not incorporate the cross correlation[28] between the solute and solvent dipole moments, $\langle \delta\mathbf{M}_0 \cdot \delta\mathbf{M}_s \rangle$. The ratio between the total and self susceptibilities determines the cavity field susceptibility equal to the ratio of the field E_c inside the solute void (cavity field[41]) to the field of external charges[11]

$$\chi_c = \frac{\chi_0}{\chi_{00}} = \frac{E_c}{E_0} \tag{12}$$

There exist two analytical results for the susceptibility χ_c established in the theory of dielectrics, the Maxwell (or Onsager[42]) cavity field and the Lorentz virtual cavity field.[30] The former considers the physical void inside the dielectric placed in a uniform electric field. The polarization of the interface creates the interface dipole given by eq 7 and the corresponding screening of the external field inside the cavity

$$\chi_c^{\text{M}} = \frac{3}{2\epsilon_s + 1} \tag{13}$$

In the case of the virtual Lorentz cavity, no physical polarization of the interface is considered and the surface charge density is identically zero (no "+" and "−" in the interface in Figure 2). The result for the cavity field susceptibility is

$$\chi_c^{\text{L}} = \frac{\epsilon_s + 2}{3\epsilon_s} \tag{14}$$

There is no screening of the external field in the Lorentz cavity (superscript "L") and only a reduction of the external field by a factor of three occurs in the limit of a highly polar solvent, $\epsilon_s \gg 1$.

The importance of the difference between $\langle (\delta\mathbf{M}_0)^2 \rangle$ in eq 11 and $\langle \delta\mathbf{M}_0 \cdot \delta\mathbf{M} \rangle$ in eq 10 can be illustrated by the example of a spherical region with the volume Ω_0 arbitrarily chosen from bulk liquid. The longitudinal response to the external field defines uniform polarization[43] $P = (\epsilon_s - 1)/(4\pi\epsilon_s)E_0$, which is also the polarization of the liquid in the slab geometry of the dielectric experiment. The polarization of the spherical region within the liquid also follows from the perturbation theory[44]

$$\frac{\epsilon_s - 1}{4\pi\epsilon_s} E_0 = \frac{\beta}{3\Omega_0} \langle \delta\mathbf{M}_0 \cdot \delta\mathbf{M} \rangle E_0 \tag{15}$$

By substituting the Maxwell χ_c^{M} in this equation to connect $\langle \delta\mathbf{M}_0 \cdot \delta\mathbf{M} \rangle$ to $\langle (\delta\mathbf{M}_0)^2 \rangle$ (eqs 10, 11, and 12), one arrives at the Kirkwood-Onsager equation[30,43,45]

$$\frac{(\epsilon_s - 1)(2\epsilon_s + 1)}{9\epsilon_s} = \frac{4\pi\beta}{9\Omega_0} \langle (\delta\mathbf{M}_0)^2 \rangle \tag{16}$$

The derivation of the dielectric constant of a liquid by Onsager shrinks the volume Ω_0 to a single molecule,[42] thus missing the Kirkwood correlation factor.[30] In contrast, cross-correlations between the dipoles on the microscopic scale lead to the microscopic form for the cavity field susceptibility. Further, the textbook derivation of the Kirkwood-Onsager equation for a spherical volume (eq 16) requires this specific shape in order to replace cross-correlations between the dipoles inside and outside the sphere with the known solution for the cavity field.

We will not assume any specific form for the cavity field susceptibility and instead will use eq 12 with the input from MD simulations. The knowl-

edge of χ_c, in turn, gives access to the interface dipole moment $\langle \mathbf{M}_{\rm int} \rangle_E$ and to the interface susceptibility $\chi_{\rm int}$ in eq 9. It is proportional to the deviation of χ_c from its Lorentz limit[11]

$$\frac{4\pi}{3}\chi_{\rm int} = \frac{3}{2(\epsilon_s - 1)}\left[\chi_c - \chi_c^{\rm L}\right] \qquad (17)$$

When the cavity susceptibility is close to the Lorentz limit, no interfacial polarization is created and the interface dipole $\langle \mathbf{M}_{\rm int} \rangle_E$ tends to zero. It is nearly impossible to predict *a priori* what kind of interfacial polarization will be created at the highly heterogeneous protein-water interface. This problem is approached here by atomistic MD simulations described below. Before we turn to the MD results, we first present the final expression for the DEP susceptibility.

By combining eqs 1, 2, and 8 with the definitions of the corresponding dipolar susceptibilities, one can arrive at the following expression[11] for the DEP susceptibility K in eq 2

$$K = \frac{\epsilon_s + 2}{3} y_p + \left[\chi_c - \chi_c^{\rm L}\right]\left(\epsilon_s y_p + \frac{3\epsilon_s}{2(\epsilon_s - 1)}\right) \qquad (18)$$

Here,

$$y_p = y_e + y_0 \qquad (19)$$

is the effective polarity[38,46] of the protein as measured by the combination of the variance of its dipole moment

$$y_0 = (4\pi/3)\chi_{00} \qquad (20)$$

and the polarity parameter y_e quantifying the density of induced dipoles in the protein molecule. This parameter is usually determined by connecting it to the refractive index of the protein n_p through the Clausius-Mossotti equation

$$\frac{n_p^2 - 1}{n_p^2 + 2} = \frac{1}{\eta_p} y_e \qquad (21)$$

Here, η_p is the packing fraction of the protein molecules in the powder used to measure the refractive index. The common approximation is $\eta_p \simeq 1$, as was also used in Onsager's theory of dielectrics when accounting for the effects of molecular polarizability.[42]

The Maxwell and Lorentz results follow from from eq 18 and the specific forms for the cavity susceptibility in eqs 13 and 14. In the former case, one obtains

$$K^{\rm M} = \frac{3\epsilon_s}{2\epsilon_s + 1} y_p - \frac{\epsilon_s - 1}{2\epsilon_s + 1} \qquad (22)$$

This equation allows both positive, $K^{\rm M} > 0$, and negative, $K^{\rm M} < 0$, DEP depending on the values of the solvent dielectric constant and the solute polarity parameter y_p. In contrast, the Lorentz limit allows only a positive DEP with

$$K^{\rm L} = \frac{\epsilon_s + 2}{3} y_p \qquad (23)$$

Note that $K^{\rm M}$ in eq 22 returns to eq 3 with $\epsilon_0 = 1$ when $y_p \to 0$.

The opposite limit of $y_p \gg 1$ is more relevant for proteins in solution. We find from the simulations of cytochrome *c* that $y_p \simeq 40 - 70$ at $T > 300$ K. Given that the static dielectric constant of water $\epsilon_s \simeq 78$ is also very high, one can simplify eq 18 to

$$K = \epsilon_s \chi_c y_p \qquad (24)$$

We find below that neither Maxwell nor Lorentz limits describe the low-frequency DEP. However, dipolar susceptibilities considered here enter other observables as well. For instance, absorption of radiation is based on essentially the same dipolar susceptibilities as the DEP. The Lorentz limit for the cavity field (eq 14) was found to describe the absorption of THz radiation by protein solutions.[38]

Equation 24 is also fully consistent with eq 3 when the standard rules for the electrostatics of interfaces apply. We consider here an ideal gas of non-interacting solutes allowing an exact relation between y_p and the effective dielectric constant of such an ensemble of dipoles. Since solute dipoles are immersed in the dielectric medium with the dielectric constant ϵ_s, all results for the ideal gas of dipoles can be used upon replacing ϵ_0 with ϵ_0/ϵ_s (only the ratio of the dielectric constants enter the dielectric boundary-value problem[2]). One therefore obtains[29] $3y_p = \epsilon_0/\epsilon_s - 1$. Similarly, eq 13 for the Maxwell reaction field becomes $\chi_c = 3/(2\epsilon_s + \epsilon_0)$. Combining these two results in eq 24 leads to eq 3.

Our MD simulations discussed below produce values of K significantly higher than the upper bound $K \equiv 1$ suggested by eq 3. The reason for the discrepancy, as pointed out above, is that the statistics of arrival of dipoles to the interface (dividing surface) is dictated by the local structure and is different from the rules established for two macroscopic dielectrics in contact. In other words, the Maxwell boundary-value problem does not apply to the the interfacial polarization induced by the external field in the protein-water interface. Specifically for the present problem, the cavity field susceptibility χ_c deviates strongly from the prediction of Maxwell's electrostatics.[11,41]

Molecular dynamics simulations

Here we calculate the cavity susceptibility χ_c and the solute polarity parameter y_0 from MD simulations of cytochrome *c* heme protein in TIP3P water. The simulation protocol was described in more detail elsewhere.[47,48] Briefly, we used the NMR solution structure of horse heart cytochrome *c* (PDB 1GIW) as the starting configuration for classical NVT simulations carried out with NAMD software suite.[49] The trajectory length of ≥ 250 ns was produced for each temperature using the cubic simulation box (100Å$\times$100Å$\times$100Å) containing one protein and 33231 TIP3P water molecules. An additional simulation with the added neutralizing NaCl electrolyte (0.3 mM ionic concentration) was 310 ns long. Particle mesh Ewald (12 Å cutoff) was applied to handle the long-range electrostatics. The time step of 2.0 fs was used in all simulations.

The simulation results reported here are obtained without electrolyte in the simulation box. The overall charge of the simulation box is non-zero and is equal to the charge of oxidized cytochrome *c* ($Q = +9$). This uncompensated charge does not affect the calculation of self- and cross-correlations between fluctuations of water, $\delta\mathbf{M}_s$, and protein, $\delta\mathbf{M}_0$, dipole moments. Including electrolyte in simulations of the dielectric response is a difficult technical problem since the dipole moment of the electrolyte gains discontinuous unphysical changes when ions cross the boundaries of the simulation box in simulation protocols involving periodic boundary conditions.[50] Methods adopted to study dielectric response of electrolytes include the unfolding of ionic trajectories into periodic images of the central simulation box[8] and/or using ionic currents, instead of ionic dipole moments, to construct time-dependent response functions.[51,52] Reliability of both approaches has not been tested for the calculation of cross-correlations between the protein dipole and the dipole of the ionic electrolyte, which enters χ_0 in eq 10 when the ionic component is added to water. We were not able to converge such correlations in our simulations involving charge-compensating electrolyte in the simulation box and for now leave the subject of the effect of ions on the cavity field susceptibility to future studies. We nevertheless calculated the dipolar susceptibilities χ_0 and χ_{00} from the simulation involving the neutralizing electrolyte and obtained the cavity susceptibility χ_c (eq 12) about 25% lower in magnitude than χ_c with no electrolyte in the simulation cell (Table 1 footnote). This calculation, however, does not include the self- and cross-correlations involving the dipole moment of the ions.

Dynamics produced by MD are used to extend the static calculations presented above to the frequency domain. The extensions to dynamics are usually produced in dielectric theories by replacing the static dielectric constants ϵ_0 and ϵ_s with the complex-valued frequency dependent functions $\epsilon_0(\omega)$ and $\epsilon_s(\omega)$. In terms of applying this procedure to DEP, on has to take the real part of $K(\omega)$ in eq 3.

In principle, both the solvent and the solute should possess their own dielectric dispersions related to Debye relaxation of the corresponding molecular dipoles.[53] However, the Debye peak of water at $\sim$ 18 GHz[54] is far above the usual frequency range of DEP measurements. For proteins in solution, rotational relaxation of the protein dipole is caused by tumbling of the protein on the time-scale of $\approx 10 - 20$ ns for a globular protein.[28] Since this time-scale can potentially enter the frequency window of the DEP experiment, we explicitly consider here the protein dynamics and the dynamics of the dipole moment of water coupled to the protein. This is typically not done in analyzing the DEP data where only the ionic conductivity is used to produce the frequency de-

pendent dielectric constant.[4] In our present simulations, we consider proteins in water without the presence of electrolyte. The goal here is to analyze the polar response of water and to calculate the cavity susceptibility of the protein-water interface not complicated by the effects of the ionic atmosphere. Since there is a connection between the DEP susceptibility and dielectric increment of the protein solution (eq 5) our results with the absence of electrolyte can be contrasted with experimental dielectric measurements where electrolyte is a part of the dielectric response. The effect of the ionic strength on the dielectric increment can be explored experimentally and extrapolated to the limit of zero ionic strength in order to connect with zero-electrolyte results discussed here.

Calculations in the frequency domain require dipole-dipole time correlation functions following standard recipes of the linear response theory.[40,52] Specifically, we calculate the frequency-dependent susceptibilities $\chi_0(\omega)$ and $\chi_{00}(\omega)$, which are one-sided Laplace-Fourier transforms of the corresponding time-depended susceptibility functions.[40] The results are similar for both functions and we list here only $\chi_0(\omega)$

$$\tilde{\chi}_0(\omega) = \chi_0 \left[1 + i\omega\tilde{\phi}_0(\omega)\right] \qquad (25)$$

Here, the tildes are used to distinguish the Fourier-Laplace transform from the full Fourier transform and χ_0 is the static susceptibility given by eq 10. Further, the function $\tilde{\phi}_0(\omega)$ is obtained from the normalized time correlation function

$$\phi_0(t) = [\langle \delta\mathbf{M}_0 \cdot \delta\mathbf{M}\rangle]^{-1}\langle \delta\mathbf{M}_0(t) \cdot \delta\mathbf{M}(0)\rangle \qquad (26)$$

calculated from simulations. A similar procedure is used to produce $\tilde{\chi}_{00}(\omega)$, which is based on the normalized time correlation function of the protein dipole (Figure 3)

$$\phi_{00}(t) = [\langle (\delta\mathbf{M}_0)^2\rangle]^{-1}\langle \delta\mathbf{M}_0(t) \cdot \delta\mathbf{M}_0(0)\rangle \qquad (27)$$

The use of eq 25 and a corresponding equation for $\tilde{\chi}_{00}(\omega)$ leads to the cavity susceptibility

$$\chi_c(\omega) = \tilde{\chi}_0(\omega)/\tilde{\chi}_{00}(\omega) \qquad (28)$$

The complex-valued frequency-dependent DEP susceptibility $K(\omega)$ therefore follows directly from eq 18 upon replacing χ_c with its frequency-dependent analog and using the frequency dependent dielectric function $\epsilon_s(\omega)$ for water.[54] In addition, y_p becomes a function of frequency as well,

$$y_p(\omega) = y_e + (4\pi/3)\tilde{\chi}_{00}(\omega) \qquad (29)$$

The effective polarity of the solute is thus reduced to the electronic polarizability given by y_e in the limit when the relaxation time of the solute dipole far exceeds the period of oscillations of the external field.

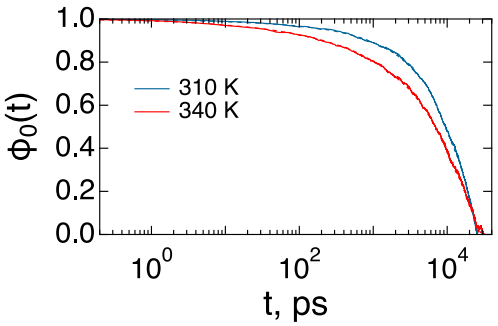

Figure 3: Time correlation functions $\phi_0(t)$ (solid lines) and $\phi_{00}(t)$ (dashed lines) calculated from MD of cytochrome *c* at the temperatures indicated in the plot. The dashed lines are indistinguishable from the solid lines on the scale of the plot.

The main results of the simulations are collected in Table 1. We list in the table the ensemble averaged dipole moment magnitude of the oxidized cytochrome *c*, which is in the range of the values from $\simeq$ 235 D to $\simeq$ 260 D[27] reported for charge $+9$ cytochrome *c* experimentally. We also list the cavity field susceptibilities χ_c calculated from MD simulations and from Lorentz and Maxwell models. As we mentioned above, the combination of a large value of χ_c with a large y_0 in eq 24 leads to a very high DEP susceptibility $K \simeq 10^3 - 10^4$.

The frequency dependence of the susceptibilities comes from the decay of the correlation functions $\phi_0(t)$ and $\phi_{00}(t)$ (eqs 26 and 27), which both are found to be essentially single-exponential with nearly equal relaxation times $\tau_R \simeq 11 - 13$ ns arising from tumbling of cytochrome *c* in solution (Table 1 and Figure 3). The overall frequency dependence of Re$[K(\omega)]$ therefore shows the standard

Table 1: Results of MD simulations for oxidized cytochrome *c* in TIP3P water.

T, K	$\langle M_0 \rangle$, D	$y_0{}^a$	χ_c	χ_c^{L}	χ_c^{M}	K	τ_R, ns
310	238	67	1.62[b]	0.34	0.02	8010	12.8
320	233	57	1.51	0.34	0.02	6033	11.7
340	216	39	1.52	0.34	0.02	4288	11.2

[a]determined from eqs 11 and 20 with the volume of cytochrome *c* protein $\Omega_0 = 27438$ Å^3. [b]cavity susceptibility $\chi_c = 1.24$ was calculated from dipolar susceptibilities from 310 ns MD simulation involving neutralizing electrolyte (0.3 mM ionic concentration). This calculation does not include the dipole moment of the electrolyte.

Debye-type drop at frequencies $\omega\tau_R \simeq 1$ in the frequency range of $\sim$ 100 MHz (Figure 4). We also note that in contrast to the static values of χ_0 and χ_{00}, which are noticeably different in their magnitudes, the dynamics of $\phi_0(t)$ and $\phi_{00}(t)$ are nearly indistinguishable (Figure 3). This observation implies that the protein is the slowest part of the entire system and water follows adiabatically its rotational tumbling.

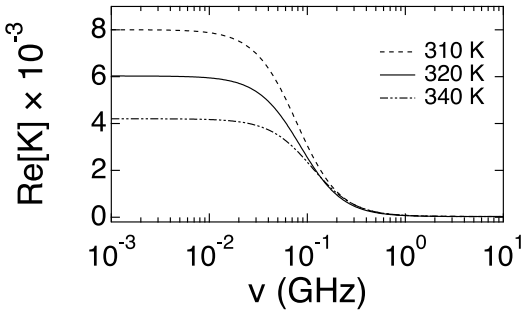

Figure 4: Re$[K(\omega)]$ for cytochrome *c* at the temperatures indicated in the plot.

In addition to a large value of the DEP susceptibility, far exceeding the standard estimates, our results show a significant dependence of the DEP effect on temperature. This result is not shared by the continuum estimates. A strong temperature dependence arises from the factor $y_p(T)$ in eq 24, which obviously scales as T^{-1} per eqs 11, 19, and 20. However, this is not the only source of change. The dipole variance $\langle(\delta\mathbf{M}_0)^2\rangle$ itself shows a substantial decrease with increasing T, as was also found experimentally,[55,56] thus enhancing the overall drop of χ_{00} and y_p (eqs 19 and 20) with increasing temperature (Table 1).

Dielectric spectroscopy of solutions

Equation 24 suggests that DEP gives access only to the product $y_p(\omega)\chi_c(\omega)$. The same two functions in fact enter the increment $\Delta\epsilon(\omega)$ of the dielectric function of a low-concentration (ideal) solution compared to the dielectric constant of the solvent. For ideal solutions, the dielectric increment is a linear function of the volume fraction η_0 occupied by the solutes. In order to derive the equation for the solution dielectric constant, we first direct the external field perpendicular to the slab of dielectric in a plane capacitor of the dielectric experiment (z-axis). The dielectric constant of the mixture (solution) ϵ_{mix} occupying the volume V with N_0 solutes can be directly found by applying the first-order perturbation theory to polarization along the z-axis[30]

$$\frac{\epsilon_{\mathrm{mix}} - 1}{4\pi\epsilon_{\mathrm{mix}}} E_0 = \frac{\epsilon_s - 1}{4\pi\epsilon_s} E_0 + \frac{\beta\langle\delta M_{0z}^2\rangle N_0}{V}\chi_c E_0 \tag{30}$$

Since we want to express the dielectric constant in terms of a spherically-symmetric dipole moment variance $\langle(\delta\mathbf{M}_0)^2\rangle$, we then direct the external field along the plane of the dielectric slab. There is no field discontinuity in this geometry[1] and the external field E_0 is equal to the Maxwell field E. One obtains

$$\frac{\epsilon_{\mathrm{mix}} - 1}{4\pi} E = \frac{\epsilon_s - 1}{4\pi} E + \frac{\beta\langle\delta M_{0x}^2\rangle N_0}{V}\chi_c E \tag{31}$$

where the x-axis is chosen in the plane of the dielectric slab.

We next combine eqs 30 and 31 to form the variance of the solute dipole $\langle(\delta\mathbf{M}_0)^2\rangle = \langle\delta M_{0z}^2\rangle + 2\langle\delta M_{0x}^2\rangle$. Expanding the result in the small param-

eter $\Delta\epsilon/\epsilon_s \ll 1$ ($\Delta\epsilon = \epsilon_{\rm mix} - \epsilon_s$), one gets

$$\Delta\epsilon(\omega) \simeq 9\eta_0 y_0(\omega)\chi_c(\omega)\epsilon_s(\omega)^2\left[2\epsilon_s(\omega)^2+1\right]^{-1} \simeq (9/2)\eta_0 y_0(\omega)\chi_c(\omega) \quad (32)$$

where the volume fraction is $\eta_0 = \Omega_0 N_0/V$ and $y_0(\omega) \gg y_e$ at low frequencies was adopted. The DEP susceptibility $K(\omega)$ in eq 5 follows from this equation and eq 24.

The parameter $\delta = \Delta\epsilon/c$, where c is the protein concentration in mg/cm^3 is often reported from dielectric measurements.[5,20,26,57,58] One can produce an estimate of the dipole moment of the protein from the parameter δ assuming a rigid protein dipole M_0, which is not affected by elastic shape fluctuations: $\langle(\delta M_0)^2\rangle = M_0^2$. From eq 32 at $\omega \to 0$ one gets

$$M_0 = \sqrt{\frac{mk_{\rm B}T}{2\pi\chi_c N_A}\delta} \quad (33)$$

where the molar mass of the protein m is in kilodaltons and N_A is the Avogadro number. By substituting the constants, this equation can be written at $T = 300$ K in units of debyes

$$M_0 = 105\,{\rm D}\,\sqrt{m\delta/\chi_c} \quad (34)$$

Equation 33 is nearly identical to the widely used Oncley formula,[21]

$$M_0^{\rm O} = \sqrt{\frac{9m}{4\pi b N_A}k_{\rm B}T\delta} \quad (35)$$

where b, in Oncley's formulation, is the parameter responsible for the cavity field correction. This assignment is fully consistent with our formulation, which requires $b = (9/2)\chi_c$. Oncley further notes that b depends on the model used to describe the cavity field and accepts an empirical value $b \simeq 5.8$ based on applying his equation to amino acids with known dipole moments.[5,21] With this parameter adopted in eq 35, Oncley's equation becomes

$$M_0^{\rm O} = \sqrt{\frac{m}{2.58\pi N_A}k_{\rm B}T\delta} \quad (36)$$

Whether the same empirical calibration applies equally well to proteins has never been established. However, Oncley's result converges to our formulation when adopting $2\chi_c \simeq 2.58$. This empirical outcome is in fact reasonably consistent with the MD results listed in Table 1. Our simulations therefore provide computational underpinning for the empirical Oncley formula.

Empirical evidence suggests that Oncley's equation often yields reasonable estimates of the protein dipole based on δ parameters from dielectric measurements.[26,59] As an example, South and Grant[57] report $\delta \simeq 0.15$ (cm^3/mg) for solutions of horse myoglobin at ambient conditions. From this number, eq 36 gives $M_0 \simeq 154$ D. Likewise, applying $\delta \simeq 0.52$ (cm^3/mg) for cytochrome c[59] and χ_c from Table 1, one obtains from eq 33 $M_0 \simeq 210$ D, not too far from direct calculations of the dipole moment listed in Table 1. This consistency with the dielectric data strongly supports the high values of the DEP susceptibility listed in Table 1 and points to the failure of the Clausius-Mossotti factor in eq 3.

If the Maxwell approximation for the cavity field susceptibility is applied, one has $\chi_c = \chi_c^{\rm M} \simeq 3/(2\epsilon_s)$ and

$$M_0^{\rm M} = \sqrt{\frac{\epsilon_s m}{3\pi N_A}k_{\rm B}T\delta} \quad (37)$$

It is clear that the direct application of the Maxwell cavity field should lead to significantly higher estimates for the protein dipole moment, $M_0^{\rm M} \simeq M_0\sqrt{\epsilon_s}$.

There are a number of complications which do not allow to access the accuracy of the Oncley formula, potentially leading to discrepancies between the results reported for the same protein. For instance, 122 D[56] and 208 D[34] have been recently reported for lysozyme from very similar analyzing protocols. It is not clear if different cavity susceptibilities apply in each case or the reported values have been affected by strong dipolar correlations between proteins in solution.[25] Potentially important are effects of the electrolyte on the cavity susceptibility χ_c, which have not been analyzed in this study. One might anticipate that electrolyte will reduce the value of χ_c due to screening of the surface charge. The results reported in Table 1 likely represent the upper bound for χ_c. Nevertheless, the agreement between the dipole moments of cy-

tochrome *c* extracted from the dielectric increment (eq 33) and from atomic charges suggests that the effect of electrolyte on χ_c is of minor importance.

Discussion

Dielectric response of a liquid in contact with a nanometer-scale interface or in the nanometer-scale confinement is significantly different from the dielectric response of the bulk.[60–66] Recent measurements of the dielectric constant of water placed in nanometer channels and in surface contact with graphite[67] have shown that the dielectric constant might be as low as ≈ 2.1 within the layer of water $\approx$ 7 Å thick. The explanation of these obseravtions that water dipoles are nearly immobile in the first two hydration layers contradicts to simulations. A more plausible explanation is that the dielectric response in the interface is highly anisotropic,[7,62,68] with a very low dipolar susceptibility along the normal to the surface. The water dipoles in contact with hydrophobic substrates tend to orient their dipoles parallel to the dividing surface.[69] The dielectric response and corresponding fluctuations of the dipole in that parallel directions are actually large.[7,65,68] However, it is the direction normal to the dividing surface that only matters for the dielectric response,[7,70] and the corresponding dielectric susceptibility is low, in agreement with experiment.[67]

A low dipolar susceptibility of the hydration shell dipoles leads to observable consequences consistent with the Lorentz construction for the cavity field inside a void or a nonpolar solute placed in a polarized dielectric[41,71] The basic physical meaning of the Lorenz construction is that the surface charge at the dividing surface (Figure 2) tends to zero, in contrast to the Maxwell dielectric boundary-value problem (eq 7). What is the basic picture of the surface dipolar polarization and the corresponding dipolar susceptibility at the protein-water interface is still mostly unknown. Absorption of radiation at THz frequencies[35] is also consistent with the Lorentz picture[37,38] of essentially no susceptibility in the direction normal to the surface (and no surface charge, Figure 2). The orientations of water dipoles in the interface are highly disordered, leading to nearly zero net projection on the normal direction at the dividing surface.[72] However, susceptibilities at lower frequencies have not been reported experimentally. This study is a step toward filling this gap by producing experimentally testable predictions by using numerical MD simulations.

The present study confirms the earlier result[11] that the cavity field susceptibility, calculated as the ratio of the full (eq 10) and self (eq 11) correlation functions of the protein dipole, is substantially higher than both the Lorentz and Maxwell predictions, although closer to the Lorentz limit. This cavity susceptibility represents correlations of fluctuations of molecular charges of the protein with molecular dipoles of the hydration shell. A high χ_c practically means that no substantial screening of protein charges is produced by the hydration shell. In addition to the hydration shell, electrolyte is expected to follow the protein motions and screen the protein fluctuations. The extent of this screening, potentially leading to a reduction of χ_c, has not been evaluated in this study. However, the values of χ_c from simulations combined with experimental dielectric increments[59] yield dipole moments consistent with direct calculations. This outcome makes us believe that the effect of electrolyte on the cavity field susceptibility is of minor importance. The large values of the DEP susceptibility, $K \approx (4-8)\times 10^3$, reported here are consistent with the dielectric data. We conclude that the Clausius-Mossotti factor (eq 3), predicting much smaller DEP susceptibility $K < 1$, is inadequate for describing the protein DEP.

Author Information:
Corresponding author: *dmitrym@asu.edu
Notes: The authors declare no competing financial interest.

Acknowledgement This research was supported by the National Science Foundation (CHE-1800243). CPU time was provided by the National Science Foundation through XSEDE resources (TG-MCB080071).

References

(1) Jackson, J. D. *Classical Electrodynamics*; Wiley: New York, 1999.

(2) Landau, L. D.; Lifshitz, E. M. *Electrodynamics of Continuous Media*; Pergamon: Oxford, 1984.

(3) Jones, T. B. *Electromechanics of Particles*; Cambridge University Press: Cambridge, 1995.

(4) Pethig, R. Review article—dielectrophoresis: Status of the theory, technology, and applications. *Biomicrofluidics* **2010**, *4*, 022811–35.

(5) Pethig, R. *Dielectrophoresis. Theory, Methodology and Biological Applications*; Wiley, 2017.

(6) Cametti, C. Dielectric properties of soft-particles in aqueous solutions. *Soft Matter* **2011**, *7*, 5494–5506.

(7) Matyushov, D. V. Electrostatics of liquid interfaces. *J. Chem. Phys.* **2014**, *140*, 224506.

(8) Yang, L.; Weerasinghe, S.; Smith, P. E.; Pettitt, B. M. Dielectric response of triplex DNA in ionic solution from simulations. *Biophys. J.* **1995**, *69*, 1519–1527.

(9) Simonson, T. Electrostatics and dynamics of proteins. *Rep. Prog. Phys.* **2003**, *66*, 737–787.

(10) Cuervo, A.; Dans, P. D.; Carrascosa, J. L.; Orozco, M.; Gomila, G.; Fumagalli, L. Direct measurement of the dielectric polarization properties of DNA. *Proc. Natl. Acad. Sci. U.S.A.* **2014**, *111*, E3624–E3630.

(11) Matyushov, D. V. Dipolar response of hydrated proteins. *J. Chem. Phys.* **2012**, *136*, 085102.

(12) Washizu, M.; Suzuki, S.; Kurosawa, O.; Nishizaka, T.; Shinohara, T. Molecular dielectrophoresis of biopolymers. *IEEE Trans. Ind. Appl.* **1994**, *30*, 835.

(13) Lapizco-Encinas, B. H.; Ozuna-Chacón, S.; Rito-Palomares, M. Protein manipulation with insulator-based dielectrophoresis and direct current electric fields. *J. Chromatogr. A* **2008**, *1206*, 45–51.

(14) Laux, E.-M.; Knigge, X.; Bier, F. F.; Wenger, C.; Hölzel, R. Dielectrophoretic immobilization of proteins: Quantification by atomic force microscopy. *ELECTROPHORESIS* **2015**, *36*, 2094–2101.

(15) Nakano, A.; Ros, A. Protein dielectrophoresis: Advances, challenges, and applications. *ELECTROPHORESIS* **2013**, *34*, 1085–1096.

(16) Pethig, R. Review—where is dielectrophoresis (DEP) going? *J. Electrochem. Soc.* **2017**, *164*, B3049–B3055.

(17) Castellanos, A.; Ramos, A.; González, A.; Green, N. G.; Morgan, H. Electrohydrodynamics and dielectrophoresis in microsystems: scaling laws. *J. Phys. D: Appl. Phys.* **2003**, *36*, 2584–2597.

(18) Nakano, A.; Chao, T.-C.; Camacho-Alanis, F.; Ros, A. Immunoglobulin G and bovine serum albumin streaming dielectrophoresis in a microfluidic device. *ELECTROPHORESIS* **2011**, *32*, 2314–2322.

(19) Barlow, D. J.; Thornton, J. M. Charge distribution in proteins. *Biopolymers* **1986**, *25*, 1717–1733.

(20) Grant, E. H.; Sheppard, R. J.; South, G. P. *Dielectric Behaviour of Biological Molecules in Solution*; Clarendon Press: Oxford, 1978.

(21) Oncley, J. L. The investigation of proteins by dielectric measurements. *Chem. Rev.* **1942**, *30*, 433–450.

(22) Pethig, R. Protein-water interactions determined by dielectric methods. *Annu. Rev. Phys. Chem.* **1992**, *43*, 177–205.

(23) Antosiewicz, J. Computation of the dipole moments of proteins. *Biophysical Journal* **1995**, *69*, 1344–1354.

(24) Takashima, S. Electric dipole moment of globular proteins: measurement and calculation with NMR and X-ray databases. *J. Non-crystal. Solids* **2002**, *305*, 303–310.

(25) Oleinikova, A.; Sasisanker, P.; Weingärtner, H. What can really be learned from dielectric spectroscopy of protein solutions? A case study of Ribonuclease A. *J. Phys. Chem. B* **2004**, *108*, 8467.

(26) Mellor, B. L.; Cruz Cortés, E.; Busath, D. D.; Mazzeo, B. A. Method for estimating the internal permittivity of proteins using dielectric spectroscopy. *J. Phys. Chem. B* **2011**, *115*, 2205–2213.

(27) Koppenol, W. H.; Rush, J. D.; Mills, J. D.; Margoliash, E. The dipole moment of cytochrome c. *Mol. Biol. Evol.* **1991**, *8*, 545–558.

(28) Boresch, S.; Höchtl, P.; Steinhauser, O. Studying the dielectric properties of a protein solution by computer simulation. *J. Phys. Chem. B* **2000**, *104*, 8743.

(29) Fröhlich, H. *Theory of Dielectrics*; Oxford University Press: Oxford, 1958.

(30) Böttcher, C. J. F. *Theory of Electric Polarization, Vol. 1: Dielectrics in Static Fields*; Elsevier: Amsterdam, 1973.

(31) Matyushov, D. V. On the theory of dielectric response of protein solutions. *J. Phys.: Cond. Matter* **2012**, *24*, 325105.

(32) Rupley, J. A.; Gratton, E.; Careri, G. Water and globular proteins. *Tr. Biochem. Scie.* **1983**, *8*, 18–22.

(33) Khodadadi, S.; Sokolov, A. P. Protein dynamics: from rattling in a cage to structural relaxation. *Soft Matter* **2015**, *11*, 4984–4998.

(34) Cametti, C.; Marchetti, S.; Gambi, C. M. C.; Onori, G. Dielectric relaxation spectroscopy of lysozyme aqueous solutions: Analysis of the delta-dispersion and the contribution of the hydration water. *J. Phys. Chem. B* **2011**, *115*, 7144–7153.

(35) Ebbinghaus, S.; Kim, S. J.; Heyden, M.; Yu, X.; Heugen, U.; Gruebele, M.; Leitner, D. M.; Havenith, M. An extended dynamical hydration shell around proteins. *Proc. Natl. Acad. Sci.* **2007**, *104*, 20749–20752.

(36) Charkhesht, A.; Regmi, C. K.; Mitchell-Koch, K. R.; Cheng, S.; Vinh, N. Q. High-precision megahertz-to-terahertz dielectric spectroscopy of protein collective motions and hydration dynamics. *J. Phys. Chem. B* **2018**, *122*, 6341–6350.

(37) Heyden, M.; Tobias, D. J.; Matyushov, D. V. Terahertz absorption by dilute aqueous solutions. *J. Chem. Phys.* **2012**, *137*, 235103.

(38) Martin, D. R.; Matyushov, D. V. Terahertz absorption of lysozyme in solution. *J. Chem. Phys.* **2017**, *146*, 084502.

(39) Matyushov, D. V. Electrophoretic mobility without charge driven by polarisation of the nanoparticle–water interface. *Mol. Phys.* **2014**, *112*, 2029–2039.

(40) Hansen, J.-P.; McDonald, I. R. *Theory of Simple Liquids*, 4th ed.; Academic Press: Amsterdam, 2013.

(41) Martin, D. R.; Matyushov, D. V. Cavity field in liquid dielectrics. *Europhys. Lett.* **2008**, *82*, 16003.

(42) Onsager, L. Electric moments of molecules in liquids. *J. Am. Chem. Soc.* **1936**, *58*, 1486–1493.

(43) Madden, P.; Kivelson, D. A consistent molecular treatment of dielectric phenomena. *Adv. Chem. Phys.* **1984**, *56*, 467–566.

(44) Høye, J. S.; Stell, G. Statistical mechanics of polar systems. II. *J. Chem. Phys.* **1976**, *64*, 1952–1966.

(45) Kirkwood, J. G. The dielectric polarization of polar liquids. *J. Chem. Phys.* **1939**, *7*, 911–919.

(46) Stell, G.; Patey, G. N.; Høye, J. S. Dielectric constants of fluid models: Statistical mechanical theory and its quantitayive implementation. *Adv. Chem. Phys.* **1981**, *48*, 183–328.

(47) Dinpajooh, M.; Martin, D. R.; Matyushov, D. V. Polarizability of the active site of cytochrome *c* reduces the activation barrier for electron transfer. *Sci. Rep.* **2016**, *6*, 28152.

(48) Seyedi, S.; Matyushov, D. V. Termination of biological function at low temperatures: Glass or structural transition? *J. Phys. Chem. Lett.* **2018**, *9*, 2359–2366.

(49) Phillips, J. C.; Braun, R.; Wang, W.; Gumbart, J.; Tajkhorshid, E.; Villa, E.; Chipot, C.; Skeel, R. D.; Kalé, L.; Schulten, K. Scalable molecular dynamics with NAMD. *J. Comput. Chem.* **2005**, *26*, 1781–1802.

(50) De Leeuw, S. W.; Perram, J. W. Computer simulation of ionic systems. Influence of boundary conditions. *Physica A* **1981**, *107*, 179–189.

(51) Chandra, A.; Patey, G. N. Dielectric relaxation of electrolyte solutions: Molecular dynamics and theoretical results for ions in simple dipolar solvents. *J. Chem. Phys.* **1994**, *100*, 8385–8391.

(52) Schröder, C.; Steinhauser, O. In *Computational Spectroscopy: Methodas, Experiments and Applications*; Grunenberg, J., Ed.; WILEY-VCH Verlag: Weinheim, 2010.

(53) Böttcher, C. J. F. *Theory of electric polarization*; Elsevier, 1973; Vol. 2.

(54) Vinh, N. Q.; Sherwin, M. S.; Allen, S. J.; George, D. K.; Rahmani, A. J.; Plaxco, K. W. High-precision gigahertz-to-terahertz spectroscopy of aqueous salt solutions as a probe of the femtosecond-to-picosecond dynamics of liquid water. *J. Chem. Phys.* **2015**, *142*, 164502–8.

(55) Bonincontro, A.; De Francesco, A.; Onori, G. Temperature-induced conformational changes of native lysozyme in aqueous solution studied by dielectric spectroscopy. *Chem. Phys. Lett.* **1999**, *301*, 189–192.

(56) Wolf, M.; Gulich, R.; Lunkenheimer, P.; Loidl, A. Relaxation dynamics of a protein solution investigated by dielectric spectroscopy. *Biochim. Biophys. Acta (BBA) - Proteins & Proteomics* **2012**, *1824*, 723–730.

(57) South, G. P.; Grant, E. H. Dielectric dispersion and dipole moment of myoglobin in water. *Proc. R. Soc. Lond. A* **1972**, *328*, 371–387.

(58) Feldman, Y. D.; Fedotov, V. D. Dielectric relaxation, rotational diffusion and the heat denaturation transition in aqueous solutions of RNAse A. *Chem. Phys. Lett.* **1988**, *143*, 309–312.

(59) Takashima, S.; Asami, K. Calculation and measurement of the dipole moment of small proteins: Use of protein data base. *Biopolymers* **1993**, *33*, 59–68.

(60) Yeh, I.-C.; Berkowitz, M. L. Dielectric constant of water at high electric fields: Molecular dynamics study. *J. Chem. Phys.* **1999**, *110*, 7935–7942.

(61) Nandi, N.; Bhattacharyya, K.; Bagchi, B. Dielectric relaxation and solvation dynamics of water in complex chemical and biological systems. *Chem. Rev.* **2000**, *100*, 2013.

(62) Stern, H. A.; Feller, S. E. Calculation of the dielectric permittivity profile for a nonuniform system: Application to a lipid bilayer simulation. *J. Chem. Phys.* **2003**, *118*, 3401–3412.

(63) Feldman, Y.; Ermolina, I.; Hayashi, Y. Time Domain Dielectric Spectroscopy Study of Biological Systems. *IEEE Transactions on Dielectrics and Electrical Insulation* **2003**, *10*, 728–753.

(64) Ballenegger, V.; Hansen, J.-P. Dielectric permittivity profiles of confined polar liquids. *J. Chem. Phys.* **2005**, *122*, 114711.

(65) Friesen, A. D.; Matyushov, D. V. Local polarity excess at the interface of water with a nonpolar solute. *Chem. Phys. Lett.* **2011**, *511*, 256–261.

(66) Bonthuis, D. J.; Gekle, S.; Netz, R. R. Profile of the static permittivity tensor of water at interfaces: Consequences for capacitance, hydration interaction and ion adsorption. *Langmuir* **2012**, *28*, 7679–7694.

(67) Fumagalli, L.; Esfandiar, A.; Fabregas, R.; Hu, S.; Ares, P.; Janardanan, A.; Yang, Q.; Radha, B.; Taniguchi, T.; Watanabe, K. et al. Anomalously low dielectric constant of confined water. *Science* **2018**, *360*, 1339–1342.

(68) Gekle, S.; Netz, R. R. Anisotropy in the dielectric spectrum of hydration water and its relation to water dynamics. *J. Chem. Phys.* **2012**, *137*, 104704–12.

(69) Lee, C. Y.; McCammon, J. A.; Rossky, P. J. The structure of liquid water at an extended hydrophobic surface. *J. Chem. Phys.* **1984**, *80*, 4448–4455.

(70) Dinpajooh, M.; Matyushov, D. V. Dielectric constant of water in the interface. *J. Chem. Phys.* **2016**, *145*, 014504.

(71) Martin, D. R.; Friesen, A. D.; Matyushov, D. V. Electric field inside a "Rossky cavity" in uniformly polarized water. *J. Chem. Phys.* **2011**, *135*, 084514.

(72) Martin, D. R.; Matyushov, D. V. Dipolar nanodomains in protein hydration shells. *J. Phys. Chem. Lett.* **2015**, *6*, 407–412.

TOC Graphic